

Random Tensor Network and Holography

by

Nadie Yiluo LiTenn

A thesis

presented to the University of California, Santa Barbara

in fulfillment of the

thesis requirement for the degree of

Honor Bachelor of Science

in

Physics

Santa Barbara, California, USA, 2022

© Nadie Yiluo LiTenn 2022

Examining Committee

This thesis is approved by

Professor:

Xi Dong

Dept. of Physics, University of California, Santa Barbara

Signature:

Abstract

Tensor networks, originally coming from the condensed matter community, serve as a useful model for investigating entanglement entropy for holographic duality. In this thesis, we describe the Ryu-Takayanagi formula that started the exploration in holographic entanglement entropy, and how the random tensor network is constructed to allow the emergence of the Ryu-Takayanagi formula by mapping the second Renyi entropy to the partition function of a classical Ising model defined on the same graph as the random tensor network.

Acknowledgements

The author would like to acknowledge Dr. Xi Dong, Sean McBride, and Wayne W. Weng for their mentorship and very helpful discussions, as well as their immense help in guiding the author into this topic. The author would be completely lost in the literatures and assumptions without their helps.

The author would also like to acknowledge Dr. Tengiz Bibilashvili for years of academic advising as well as generic advice in life. As the author was procrastinating on finishing this thesis, he suggested to the author to "Spend time to finish it ASAP and put a big check mark here!" such that the author could graduate. And so the author followed this one last advice.

In addition, the author would like to acknowledge Dr. Anthony Zee for his guidance and insights in quantum field theories though he was never obligated to offer the author any mentorship. Similarly, the author would like to acknowledge Dr. Don Marolf for his comprehensive introduction into the black hole information problem along with many insights offered during office hours.

The author would like to acknowledge Hongyin Liu, Yoho, and Chacha for emotional support as well as constantly reminding the author that they have not finished the thesis, hence could not be cleared for graduation. It was very effective.

Last but not least, the author would like to thank Mom for the all the supports in the past, present, and continuing into the future. It is always strong and consistent, but often remained unseen.

Of course, it goes without saying that the author is grateful for all the friends, faculties, staffs, and cats at UC Santa Barbara and College of Creative Studies for a wonderful experience in studying physics as well as enjoying the undergraduate life. Big shoutout to whoever decided to put a college on the beach.

Table of Contents

Examining Committee	ii
Abstract	iii
Acknowledgements	iv
List of Figures	viii
1 Introduction	1
1.1 Notation	3
2 Holographic Entanglement Entropy	4
2.1 Entanglement Entropy	4
2.2 The Ryu-Takayanagi Formula	7
2.3 Restrictions of Ryu-Takayanagi	9
2.4 Derivation of Ryu-Takayanagi	9

2.5	Homology Constraint	17
2.6	Quantum Correction to Ryu-Takayanagi	20
3	Random Tensor Network	21
3.1	A Physical Setup	21
3.2	Definition of the Random Tensor Network	23
3.3	Swap Trick	28
3.4	Single Tensor	30
3.5	Large D Limit and Ryu-Takayanagi Formula	34
3.6	Going Forward with Random Tensor Network	45
	References	47

List of Figures

2.1	The rectangular surface is the boundary divided into subregion A and B , and γ_A is the minimal surface in the bulk, bounded by the same boundary of subregion A , $\partial\gamma_A = \partial A$	8
2.2	Left: representation of density matrix in terms of path integral, where we time evolve from vacuum to obtain our bra and ket states. Right: by identifying the two red sides, we obtain $\text{tr } \rho$, which is defined to be 1 for any normalized density matrix.	11
2.3	We obtain the reduced density matrix for subregion A by tracing out the degrees of freedom of B . This also corresponds to possible information that observer in A may obtain when they are ignorant of what is going on in B	12
2.4	A diagramic representation of $\text{tr}(\rho_A^2)$, where we have two copies of ρ and "stitch" together subregions accordingly. Following the purple arrows, we find a conical surplus of 4π	13

2.5	A \mathbb{Z}_2 symmetry is explicit if we represent it this way, and in the center we have a fixed point under the symmetry transformation, and this point is where the conical singularity lies. The color scheme is inherited from Figure 2.4	14
2.6	Three different cases of minimal surfaces. Left: no black hole, the two minimal surfaces, γ_A and γ_B , coincide in the bulk. Middle: when a black hole is present, one possible way is to have γ_A and γ_B being homotopic to the boundary subregions, meaning that they can be smoothly deformed to the boundary. This is the case where two minimal surfaces don't coincide in the bulk. Right: the two minimal surfaces are homologous to their respective boundary subregions, and they coincide in the bulk. When a black hole is present, we pick between the case that gives the minimum in calculating the entanglement entropy.	19
3.1	Left: three machines that produce three Bell pairs, with David taking one photon from each pair and making a complete measurement. Right: the triangular random tensor network diagram that corresponds to the situation on the left, where David is the triangle in the bulk and the rest are dangling legs on the boundary.	23
3.2	A single tensor with n indices, represented by n legs. Each leg is represented by μ_k , which run from 1 to D_k , where D_k is the dimension of the Hilbert space endowed on that leg.	24

3.3	A simple two-tensor network, whose internal leg has dimension D_{xy} , and is projected onto the maximally entangled state in $\mathcal{H}_{xy} \otimes \mathcal{H}_{yx}$	25
3.4	Left: single tensor network. Note that we have two dangling legs for one vertex here. A single tensor with one dangling leg would be useless as we want to divide our boundary region into two for entanglement entropy calculation. Right: plugging a bulk state $ \psi_b\rangle$ to the network such that it becomes a kind of bulk to boundary mapping. The bulk state does not have to be a pure state.	26
3.5	Left: a two-tensor network with the bulk state plugged to both tensors. Right: we could combine the internal legs in the network and the bulk state, considering them as one such that effectively the tensors are independently mapping the bulk to respective boundary legs.	27
3.6	A single tensor with two dangling legs, each endowed with a Hilbert space of dimension D_A and D_B respectively.	31
3.7	A visualization of density matrix and its variations for a single tensor . . .	31
3.8	Swapping the ket legs of subregion A in the two copies.	32
3.9	Tracing over the networks after the swap operation. We can see that this diagram is the same as Figure 3.7 if we trace the lines.	33
3.10	Entanglement entropy calculated from randomly sampling the node for a single tensor in comparison to expected Page curve result.	35

- 3.11 Top: the two copies of kets for two-tensor network. Note that in reality we have two copies of density matrices, but we omit the bra here as they are irrelevant here. The swap operators only act on the kets. Middle: the kets as acted on by X_1 the swap operator at site 1. Bottom: the kets as acted on by $X_A X_1$. We see that as viewed from the boundary, this is effectively the same as the top panel. The boundary does not observe the crossing in the boundary leg because no information is shared between the boundary and the boundary nodes, unlike the internal legs, whose information is shared through the projection onto $|xy\rangle$ for nearby nodes x and y . The crossing on the internal leg between site 1 and 2, however, will be seen by both nodes and will be reflected as we take a trace over those. 39
- 3.12 Left: single tensor network with bulk state. In this case, identity operator is assigned to the tensor, corresponding to a $s = +1$ spin variable on the tensor. The domain wall is through the dangling leg as we choose A to be the boundary subregion of interest, corresponding to spin down in subregion A . Right: swap operator $s = -1$ is assigned to the tensor, so the domain wall is through the dangling leg of B . In this case, we have $e^{-S_2(A)} \sim \text{tr}(\rho_P \otimes \rho_P X_B)$ so it is effectively the second Renyi entropy of ρ_P restricted to the spin down domain. 40
- 3.13 Two tensor network with a domain wall cutting through the internal leg. This configuration contributes a $\log D_{xy}$ term to the second Renyi entropy. 43

Chapter 1

Introduction

AdS/CFT correspondence is a duality between a quantum gravity system on a $(d + 1)$ dimensional asymptotically AdS space, and a d dimensional CFT on its boundary. Since its introduction [19], it has been used to sharpen our understanding toward quantum gravity. It also provided a framework to study strongly coupled quantum field theories. One remarkable feature of this duality was the one between entanglement and geometry, discovered by Ryu and Takayanagi [24, 25]. It stated that the entanglement entropy of a subregion on the boundary could be represented by the area of a minimal surface in the bulk dual, which then led to a wave of followed up works [7, 8, 11, 12, 17, 18] in understanding the relation between geometry and entanglement.

Meanwhile, techniques and advancements in condensed matter physics give rise to improvements in simulating emergent phenomena in the strongly interacting systems. The key ingredient of this includes the use of tensor networks, which serve to efficiently repre-

sent quantum many-body systems [29,30,32]. This idea was combined with entanglement renormalization [31] to formulate the Multi-scale Entanglement Renormalization Ansatz (MERA), which describes the efficient representation of certain quantum many-body states on a lattice. Building from here, it was then realized that there are some similarities between the MERA tensor networks and the AdS/CFT correspondence [27,28]. This further suggested that the emergent bulk geometry could have building blocks from the quantum entanglement in a boundary theory, and the physics of holography could be modeled by some tensor network.

We give a summary of the organization of this thesis, which is divided into two parts. In Chapter 2, we give a short review on the entanglement entropy, and we introduce the Ryu-Takayanagi formula along with its derivation under the assumption of gravity in the box. We then give a small discussion on the homology constraint when choosing the minimal surface for the Ryu-Takayanagi formula. In the end, we touch on the quantum correction term to the Ryu-Takayanagi formula as it would be relevant when discussing problem for the random tensor networks. In Chapter 3, we switch gear from holographic entanglement entropy to discuss the construct of random tensor networks. We start with a physical set up to provide intuitions for the tensor network, and then we proceed into the definitions of the random tensor network. We then give a short review on the swap trick for our later use, and we calculate a simple case of a single tensor for intuitions. Finally, we discuss how we can calculate the second Renyi entropy and map it to the partition function of a classical Ising model defined on the same graph, which allows the emergence of the Ryu-Takayanagi area formula in the random tensor network. At the end, we conclude with some existing problems in random tensor network, which calls for further investigation into this very

useful model for quantum gravity.

1.1 Notation

We will use the natural unit $\hbar = c = 1$ and the $(- + + +)$ convention for the metric. As an example, the Schwarzschild metric for black hole is

$$ds^2 = -\left(1 - \frac{r_s}{r}\right)dt^2 + \left(1 - \frac{r_s}{r}\right)^{-1}dr^2 + r^2d\Omega^2 \quad (1.1)$$

where $r_S = 2GM$ with G being the Newton's constant, and M being the mass of the black hole.

Chapter 2

Holographic Entanglement Entropy

Holographic entanglement entropy proposed by Ryu and Takayanagi was a first quantified insight into the duality between geometry in a bulk theory and entanglement on the boundary dual. Along with the Page curve [21], it opens up a mean to investigate the black hole information problem [1, 14, 23]

2.1 Entanglement Entropy

We start with a small review on the entanglement entropy, otherwise known as the the von Nuemann entropy or the fine grained entropy.

In a finite quantum mechanical system, whose density matrix is $\rho = |\psi\rangle\langle\psi|$, we can define the von Neumann entropy

$$S_{vN} = -\text{tr}(\rho \log \rho) \tag{2.1}$$

This notion has an origin from the classical Shannon entropy, which is essentially a special case that takes only the classical portion of a density matrix. Now, if we have a much larger Hilbert space, such as those for a quantum field, the above quantity becomes hard to calculate due to the log inside the trace. To aid with calculation, we introduce the Renyi entropy

$$S_n = -\frac{1}{n-1} \log \text{tr}(\rho^n) \quad (2.2)$$

where the n label means the n -th Renyi entropy. By taking the limit of $n \rightarrow 1$, we will recover the von Neumann entropy. Note that we still have a log in the Renyi entropy, but now it is outside of the trace operation, so this would be a better treatment for calculation. However, we should also note that the density matrix in quantum field theory is not an exactly well defined quantity, but it is largely believed to behave nicely and provide sensible results, so we shall charge forward.

In the above definition, Renyi entropy takes discrete values n . We can analytically continue it to all positive real numbers, allowing us to take the limit $n \rightarrow 1$

$$\begin{aligned} \lim_{n \rightarrow 1} S_n &= -\lim_{n \rightarrow 1} \frac{d}{dn} \log \text{tr}(\rho^n) \\ &= -\lim_{n \rightarrow 1} \frac{\frac{d}{dn} \text{tr} \rho^n}{(\text{tr} \rho)^n} \\ &= -\lim_{n \rightarrow 1} \frac{d}{dn} \text{tr}(e^{n \log \rho}) \\ &= -\text{tr}(\rho \log \rho) = S_{vN} \end{aligned} \quad (2.3)$$

as desired. From second to third line, we use the fact that $\text{tr} \rho = 1$ for a properly normalized

density matrix. And in the third to the last line, we use the fact that trace and derivative are both linear operator so we could exchange them.

Often time, we are interested in the subsystem of a full, pure system. Consider a full system described by the density matrix $\rho_{AB} = |\psi_{AB}\rangle\langle\psi_{AB}|$, the density matrix for the subsystem A can be obtained by performing the partial trace over the subsystem B

$$\rho_A = \text{tr}_B \rho_{AB} = \text{tr}_B |\psi_{AB}\rangle\langle\psi_{AB}| \quad (2.4)$$

From here, we can consider the following case: suppose the full system can be factorized into A and B , $|\psi_{AB}\rangle = |\psi_A\rangle \otimes |\psi_B\rangle$, then after partial tracing over B , we would still obtained a pure state. It is simple calculation, but we could also provide some intuition for it: the von Neumann entropy characterize our ignorance of a system. For a pure state, the von Neumann entropy vanishes as we understand the entire system. When a full system factorizes into A and B , they stand alone from each other. As we look at A , we would not need information from B to complete our understanding of A , hence the vanishing von Neumann entropy on the subsystem A .

Now, to the contray, if we have a bipartite system that does not factorize, the von Neumann entropy of either subsystem would not vanish, meaning that some information is stored in the other half of the system for a complete retrieval of understanding of the quantum system. If the two subsystem is maxially entangled, then we would need the entirety of both subsystems to retrieve our understanding of the quantum system.

2.2 The Ryu-Takayanagi Formula

In this section we will describe the holographic entanglement entropy proposal by Ryu and Takayanagi [24, 25]. Long before Ryu and Takayangi, it was already pointed out that the entanglement entropy of subsystem resembles the black hole entropy [4, 26]. When we consider a quantum many-body system $|\psi_{AB}\rangle$ and restrict ourself to a subsystem B , we will find the entanglement entropy of the subsystem to be

$$S_B = \kappa M^2 A \tag{2.5}$$

where κ is a constant dependent on the specific system that we study, M correspond to the UV cutoff (e.g. for a lattice with spacing a , $M \sim \frac{1}{a}$), and A is the area of the boundary between subsystem, which may or may not be disjoint.

We recognize that this shares the same area law as the black hole entropy

$$S_{bh} = \frac{1}{4} M_{pl}^2 A \tag{2.6}$$

where M_{pl} is the Planck mass. So it is as if we have a horizon-like screen in the quantum many-body system. Though we should note that this screen can be put in by hand, unlike the event horizon, which is determined by the geometry itself. A natural question is, assuming we have a quantum many body system on the boundary dual to a bulk theory, and assume that the bulk theory contains an event horizon-like screen, what surface on the boundary would correspond to this screen in the bulk, if any?

In 2006, Ryu and Takayanagi proposed a solution to this question. The idea is that

suppose we have a bulk-boundary theory, where on the boundary we have quantum fields without gravity, and in the bulk we have a quantum gravity theory. Let us denote the entire spatial boundary by AB , divide it into subregions A and B , and calculate the entanglement entropy of A . It is then proposed that the von Neumann entropy of the boundary subregion A can be given by information in the bulk

$$S_A = \frac{\text{Area}[\gamma_A]}{4G_N} \quad (2.7)$$

where γ_A is the minimal surface in the bulk that is homologous to the subregion A on the boundary, and G_N is the Newton's constant. With this setup, In the simple case of a 2+1d bulk, the minimal surface is just a geodesic.

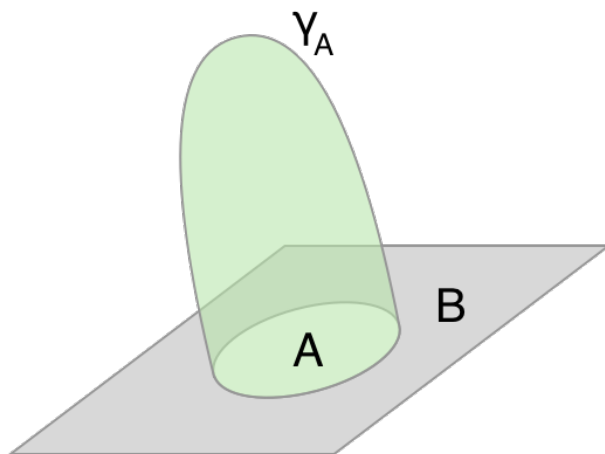


Figure 2.1: The rectangular surface is the boundary divided into subregion A and B , and γ_A is the minimal surface in the bulk, bounded by the same boundary of subregion A , $\partial\gamma_A = \partial A$

2.3 Restrictions of Ryu-Takayanagi

Ryu-Takayanagi formula is restricted in the following sense [16]: it requires the bulk theory to be classical Einstein theory and bulk spacetime to possess a time reflection symmetry under which the boundary spatial region A is invariant.

1. If we move away from classical theory, it is necessary that we include quantum correction terms, which we will discuss towards the end of part one of this review.
2. If we move away from the Einstein theory, which we consider to be an effective theory, then we will need to include higher derivative terms in the action.

$$S_{bulk} = \frac{1}{16\pi G_N^{(d+1)}} \int \sqrt{g} \left(R + \frac{d(d-1)}{l_{AdS}^2} + \sum \alpha_k \nabla^{2k} R + \mathcal{L}_{matter} \right) \quad (2.8)$$

In doing this, we are getting more "stringy", but we will not get into the details.

3. If we leave out the time reflection symmetry, we will go into, instead of a static geometry, a time dependent one. This is in fact known as the Hubeny-Rangamani-Takayanagi formula [17], but in this method a Lorentzian approach is used, so we will not discuss it in this review.

2.4 Derivation of Ryu-Takayanagi

The path integral derivation was given by Lewkowycz and Maldacena [18]. Though the full details require the framework of AdS/CFT, we shall content ourselves with a model of

gravity in the box for our derivation. So our setup is to have finite $S^2 \times \mathbb{R}$ for our boundary condition, where \mathbb{R} is the time direction. We will consider the subregion $A \subset S^2$

First, we know that we can obtain any arbitrary quantum state $|\psi\rangle$ by time evolving a vacuum state $|\Omega\rangle$ that is in the far past. And by time reflection symmetry, we can similarly obtain $\langle\psi|$ by time evolving backwards on a vacuum in the far future. With this construction, we can represent our density matrix as in Figure 2.2. We note that everything we manipulate with right now lives on the boundary. If we want to obtain the quantity $\text{tr } \rho$, we then simply identify the top and bottom sides. Therefore, in some sense, each top and bottom side represents an index of the density matrix. If there are no free top and bottom sides in the diagram (i.e. all of them are identified with another side), then we are expecting a number instead of a matrix.

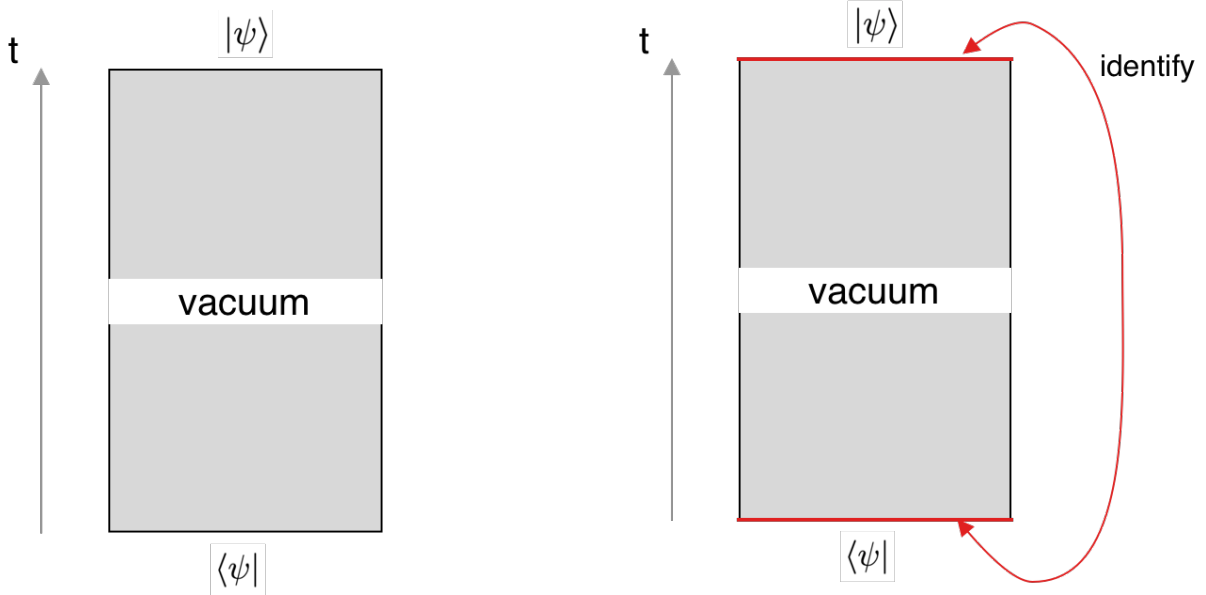


Figure 2.2: Left: representation of density matrix in terms of path integral, where we time evolve from vacuum to obtain our bra and ket states. Right: by identifying the two red sides, we obtain $\text{tr} \rho$, which is defined to be 1 for any normalized density matrix.

Our next step is to obtain the density matrix for the subregion A that we are considering. To do this, we will trace out the degrees of freedom of subregion B from the full density matrix. As before, we do a partial tracing to get the reduced density matrix ρ_A

$$\rho_A = \text{tr}_B \rho = \sum_i \langle \psi_{B,i} | \rho | \psi_{B,i} \rangle \quad (2.9)$$

This can be similarly represented with a diagram (Figure 2.3). The idea is that we identify the a subregion in the top and bottom sides.

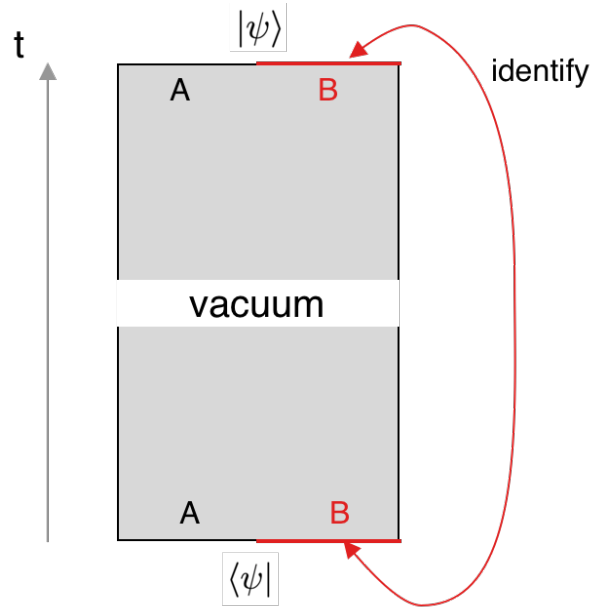


Figure 2.3: We obtain the reduced density matrix for subregion A by tracing out the degrees of freedom of B . This also corresponds to possible information that observer in A may obtain when they are ignorant of what is going on in B .

From here, it is straightforward to obtain the $\text{tr}(\rho_A^2)$ (see Figure 2.4) and similarly for $\text{tr}(\rho_A^n)$, which we shall not draw. If we follow the purple trajectory in Figure 2.4, there is a singularity corresponding to the conical surplus (more than 2π if we follow the purple arrow and go back to the starting point), that is, the boundary contains a conical singularity.

Let us pause and remind ourselves that our ultimate goal is to calculate the entanglement entropy, which requires analytic continuation of integer n in the Renyi entropy S_n to all positive real numbers. Now, it is not exactly clear what this analytic continuation means with the pictures we are working with, so we shall switch to a bulk picture instead.

We see from the above manipulation that the boundary exhibits a replica symmetry.

For example, for $n = 2$ case, we have a \mathbb{Z}_2 symmetry, which can be explicitly seen through Figure 2.5. The key is that we now have a fixed point under the replica symmetry, and this point carries the conical singularity.

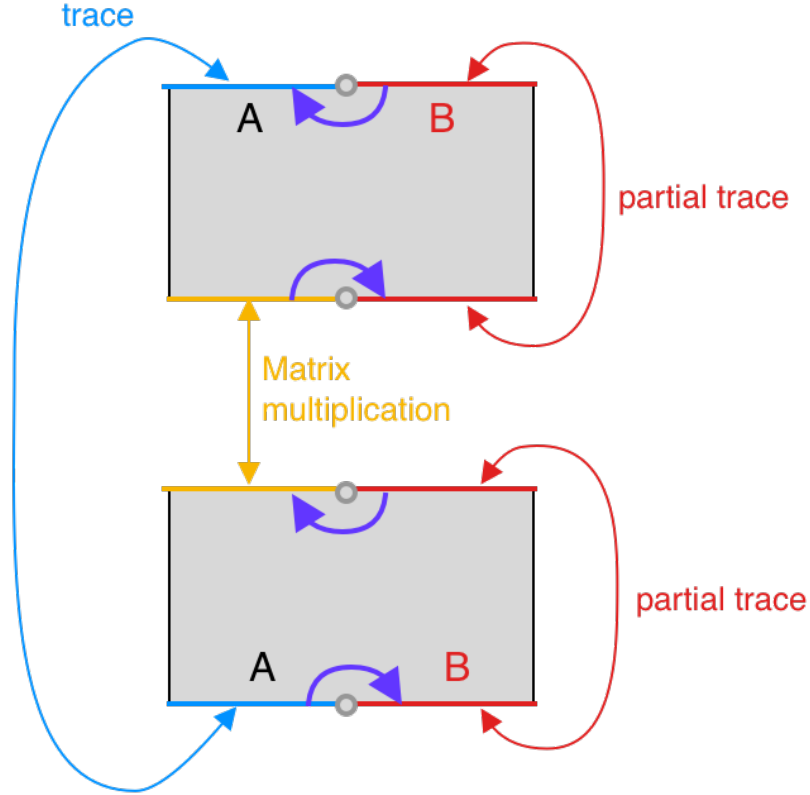


Figure 2.4: A diagrammatic representation of $\text{tr}(\rho_A^2)$, where we have two copies of ρ and "stitch" together subregions accordingly. Following the purple arrows, we find a conical surplus of 4π .

To proceed, we will make an assumption that the bulk saddles will carry the same kind of replica symmetry. So instead of working in the full bulk manifold \mathcal{M} , we can work in a quotient manifold $\tilde{\mathcal{M}}_n/\mathbb{Z}_n$, and we identify all n points under the replica symmetry. By doing so, the quotient boundary we are dealing with becomes smooth, and we have

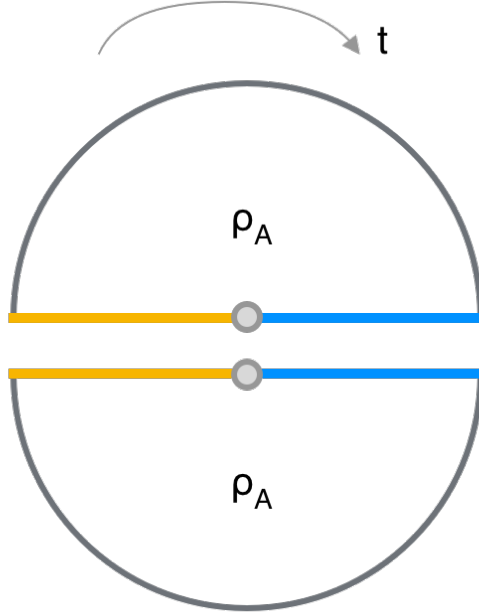


Figure 2.5: A \mathbb{Z}_2 symmetry is explicit if we represent it this way, and in the center we have a fixed point under the symmetry transformation, and this point is where the conical singularity lies. The color scheme is inherited from Figure 2.4

essentially moved the singularity into the bulk quotient space $\tilde{\mathcal{M}}_n$

Now let I_n be the Euclidean action for the full, smooth n -replica in the bulk. Under saddle point (semi-classical) approximation, we have

$$\text{tr}(\rho^n) \approx e^{-I_n} \quad (2.10)$$

where we drop the subscript A as we will exclusively be talking about the subregion.

For simplicity, we define

$$\hat{\rho} \equiv \frac{\rho}{\text{tr} \rho} \quad (2.11)$$

so we can write

$$\text{tr } \hat{\rho}^n = \frac{\text{tr } \rho^n}{(\text{tr } \rho)^n} = e^{-(I_n - nI_1)} \quad (2.12)$$

We can also define a quotient action, which integrates over the quotient space $\tilde{\mathcal{M}}_n$.

$$\tilde{I}_n \equiv \frac{I_n}{n} \quad (2.13)$$

We should however note that \tilde{I}_n is not the Einstein-Hilbert action for $\tilde{\mathcal{M}}_n$ because we have not considered contribution from the conical singularity in $\tilde{\mathcal{M}}_n$. With these notations, we can write the n -th Renyi entropy as

$$S_n = -\frac{1}{n-1} \log \hat{\rho}^n \quad (2.14)$$

$$= \frac{n}{n-1} (\tilde{I}_n - I_1) \quad (2.15)$$

We can then take the limit of $n \rightarrow 1$ to obtain the von Neumann entropy.

$$S_{vN} = \lim_{n \rightarrow 1} S_n \quad (2.16)$$

$$= \lim_{n \rightarrow 1} \frac{\tilde{I}_n - I_1}{n-1} \quad (2.17)$$

$$= \left. \frac{d}{dn} \tilde{I}_n \right|_{n=1} \quad (2.18)$$

We will pause here to think about what $\tilde{I}_n(\tilde{\mathcal{M}}_n)$ is exactly. We already know that this quantity is smooth from its definition, but the Einstein-Hilbert action for the quotient

manifold includes a term where the Ricci scalar $R(\tilde{\mathcal{M}}_n)$ gives a delta-function. So in order to get a smooth $\tilde{I}_n(\tilde{\mathcal{M}}_n)$, we need

$$\tilde{I}_n(\tilde{\mathcal{M}}_n) = I_{EH}(\tilde{\mathcal{M}}_n) + (\text{a term that cancels out the singularity}) \quad (2.19)$$

We have $I_{EH} \sim \frac{\sqrt{g}R}{16\pi G}$, where $\sqrt{g}R \sim 2\alpha\delta(\text{at singularity})$. α here is the conical defect angle. We can then write the singularity in the Einstein-Hilbert action as

$$\sim -\frac{\alpha/2\pi}{4G}\delta(\text{at singularity}) \quad (2.20)$$

After n -folding, we are left with $\frac{2\pi}{n}$ conical opening, so the conical defect is $\alpha = 2\pi(1 - \frac{1}{n})$. Here, we also see the advantage of working with the bulk picture instead of the boundary picture. Analytic continuation is more natural in the bulk, specifically from this equation, where $n \in \mathbb{R}$ just means that we have a continuous spectrum of the conical defect. Put this into above and integrate over the quotient manifold, the delta-function simply becomes the area (of the codimensions that we suppressed in our pictures) at the conical singularity. And we have the quotient action

$$\tilde{I}_n(\tilde{\mathcal{M}}_n) = I_{EH}(\tilde{\mathcal{M}}_n) + \frac{A_{conical}}{4G}(1 - \frac{1}{n}) \quad (2.21)$$

We can then substitute this back into our calculation of the von Neumann entropy to

obtain

$$S_{vN} = \left. \frac{d}{dn} \tilde{I}_n \right|_{n=1} \quad (2.22)$$

$$= \left. \frac{d}{dn} I_{EH}(\tilde{M}_n) \right|_{n=1} + \left. \frac{1}{4Gn^2} A_{conical} \right|_{n=1} + \left. \frac{1 - \frac{1}{n}}{4G} \frac{d}{dn} A_{conical} \right|_{n=1} \quad (2.23)$$

First term vanish because it is smooth and on stationary, as we are working at the saddle. The third term also vanish when we take the $n = 1$ limit, so we are left with

$$S_{vN} = \left. \frac{A_{conical}}{4G} \right|_{n=1} \quad (2.24)$$

Now we need to ponder what is $A_{conical}$ at $n = 1$. As we extremize the action to find the saddle point, we are varying the location of the conical singularity, so what we are finding is in fact the location of a surface that extremizes the von Neumann entropy.

$$S_{vN} = \frac{A(\text{extremal surface})}{4G} \quad (2.25)$$

And this concludes the path integral derivation of the Ryu-Takayanagi formula.

2.5 Homology Constraint

We should discuss briefly the homology constraint on choosing the Ryu-Takayanagi surface.

Definition 2.5.1 *We say a surface γ_A is homologous to the subregion A , denoted by $\gamma_A \sim$*

A if there exists a bulk region $r \subseteq \mathcal{M}$ such that

$$\partial r = A \cup \gamma_A \tag{2.26}$$

In this language, we can also write the Ryu-Takayanagi formula as

$$S(A) = \min_{\gamma_A \sim A} \frac{\text{Area}[\gamma_A]}{4G_N} \tag{2.27}$$

In other words, as we choose the Ryu-Takayanagi surface, we always have to follow the homology constraint. Note that this is not the same as the requirement that the surface is homotopically equivalent to the boundary region A , in which case we have a stronger condition that we must be able to smoothly deform the Ryu-Takayanagi surface to the boundary region A . In fact, homotopy condition implies the homology constraint, but not the other way.

Let us consider an example (Figure 2.6). For the case when there is no black hole in the bulk, the extremal surface γ_A and γ_B coincide in the bulk. When there is a black hole, there are two ways we can draw the Ryu-Takayanagi surface as shown in the middle and right panel in Figure 2.6. The middle panel corresponds to when we have the homotopic condition, and the right panel corresponds to when we have just the homology constraint. In the Ryu-Takayanagi formula, we choose the configuration that gives the minimum for the entanglement entropy

$$S(A) \sim \min(\text{Diagram 1}, \text{Diagram 2}) \tag{2.28}$$

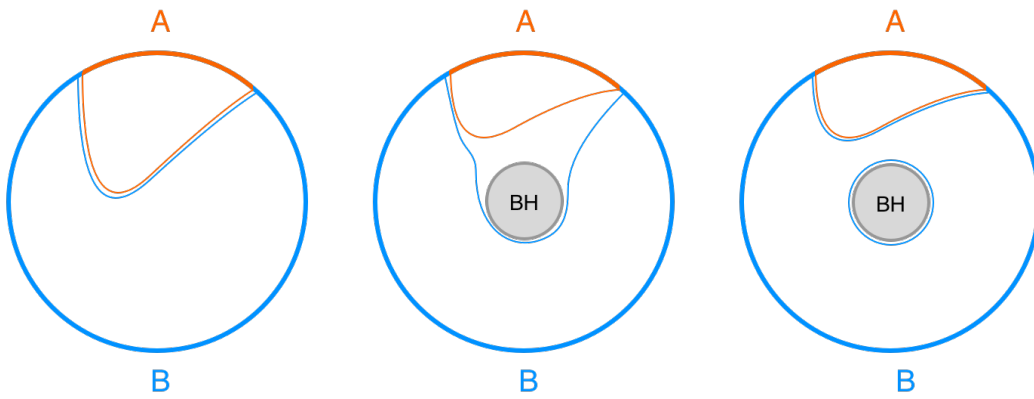


Figure 2.6: Three different cases of minimal surfaces. Left: no black hole, the two minimal surfaces, γ_A and γ_B , coincide in the bulk. Middle: when a black hole is present, one possible way is to have γ_A and γ_B being homotopic to the boundary subregions, meaning that they can be smoothly deformed to the boundary. This is the case where two minimal surfaces don't coincide in the bulk. Right: the two minimal surfaces are homologous to their respective boundary subregions, and they coincide in the bulk. When a black hole is present, we pick between the case that gives the minimum in calculating the entanglement entropy.

To be specific, we have such situation for a BTZ black hole. It might seem that we have ambiguity in choosing the Ryu-Takayanagi surface—we could also wrap around the black hole arbitrarily many times to get new surfaces homologous to the chosen boundary region. But we will only choose the minimal configuration. As we change the relevant parameter, we will have a phase transition from one configuration to another in calculating our entanglement entropy.

2.6 Quantum Correction to Ryu-Takayanagi

The Ryu-Takayanagi formula we discussed above is the $\mathcal{O}(G\hbar)^{-1}$ term for the generalized entanglement entropy, in the sense that if we take $G\hbar \rightarrow 0$, all the higher order terms shall vanish. In the context of black hole information problem [1], it is important to discuss the $\mathcal{O}(G\hbar)^n$ quantum correction term, where $n \geq 0$. It was shown by Faulkner, Lewkowycz, and Maldacena that

$$S_{vN}(R) = \frac{\text{Area}(\gamma_A)}{4G} + S_{vN}^{QFT}(\Sigma_R) + S_{\text{bulk}} \quad (2.29)$$

where Σ_R is the region bounded by γ_A and R on the boundary. A similar derivation like above can be made for the quantum correction term. However, as this is not the main focus of this thesis, we shall skip it for now and switch gear to random tensor network in the next part. We brought it up here as it will be relevant when we discuss the problems that plague the random tensor network once we are done with its basics.

Chapter 3

Random Tensor Network

It was pointed out first by Swingle that, some physics of the AdS/CFT correspondence could be modeled by a MERA-like tensor network, where quantum entanglement on the boundary become the building blocks of emergent bulk geometry [27, 28]. Later, many works explored this notion and have been successful in reproducing the Ryu-Takayanagi area law through tensor networks [22, 33], however, they are in some sense an ideal version of the large dimensional random tensors [15]. With random tensor network, we could calculate some desired properties more systematically

3.1 A Physical Setup

In this section we will detail the intuition for setting up a triangular random tensor network with three dangling legs, each from one vertex of a triangle (see Figure 3.1). This is meant for a more physical picture of the random tensor network. We will layout the

precise definitions of the random tensor network in the next section to proceed with further calculations.

First, let us consider a machine that will spit out a Bell pair, say, two maximally entangled photons. Suppose we have three of those machines. Then we can represent the initial state of the three Bell pairs by

$$|\Psi\rangle = |AD\rangle \otimes |BD\rangle \otimes |BC\rangle \tag{3.1}$$

where A , B , C , and D represent Alice, Bob, Charlie, and David in Figure 3.1 respectively.

We take one photon from each pair and assume that we will make a complete measurement on them such that the result will be a pure state $|V_a\rangle$, where a labels the possible outcomes, then the post-measurement state is

$$|\Psi_{post}\rangle = \langle V_a | \left(|AD\rangle \otimes |BD\rangle \otimes |BC\rangle \right) \tag{3.2}$$

which is the state described by the triangular random tensor network. With this setup, the entanglement is now between the three photons that have not been measured. And the three unmeasured photons are represented by the three boundary edges, sometimes referred to as dangling legs. The geometry of how these three photons are entangled is represented by the triangle in the bulk of random tensor network.

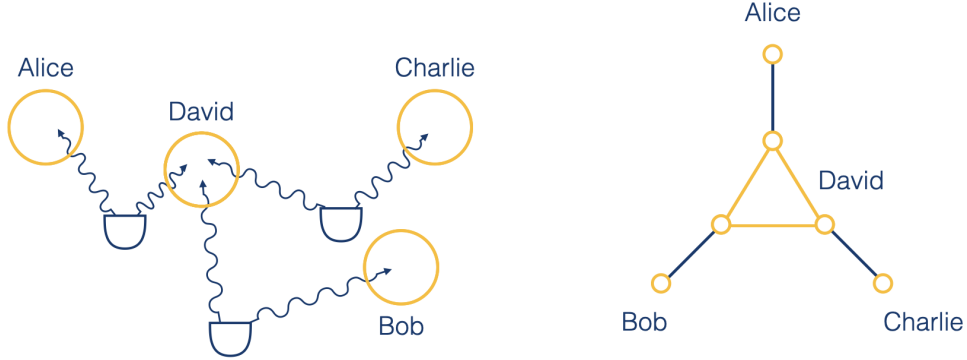


Figure 3.1: Left: three machines that produce three Bell pairs, with David taking one photon from each pair and making a complete measurement. Right: the triangular random tensor network diagram that corresponds to the situation on the left, where David is the triangle in the bulk and the rest are dangling legs on the boundary.

3.2 Definition of the Random Tensor Network

In this section, we talk about random tensor networks in a more general sense, for the convenience of later discussions.

Let us start by considering a single rank- n tensor $V_{\mu_1\mu_2\dots\mu_n}$ represented by a node V_x , and each index is represented by an edge extended from the node (see Figure 3.2). On each edge labeled by μ_k , we endow a D_k -dimensional Hilbert space \mathcal{H}_k , so μ_k runs from 1 to D_k . Note that we are dealing with a single tensor, and the edges are all dangling for now, not connected with any other nodes.

We can then write the state $|V_x\rangle$ for this single tensor

$$|V_x\rangle = \sum_{\{\mu_k\}} V_{\mu_1\mu_2\dots\mu_n} |\mu_1\rangle \otimes |\mu_2\rangle \otimes \dots \otimes |\mu_n\rangle \quad (3.3)$$

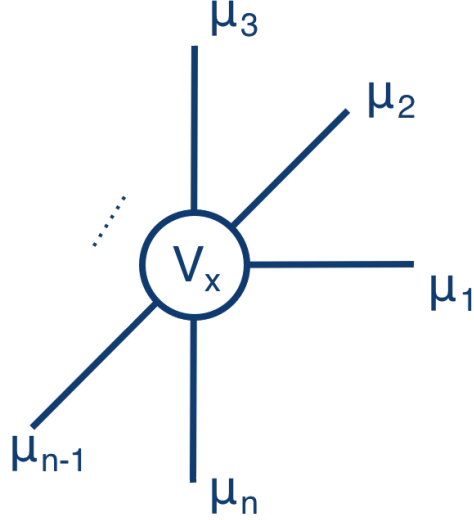


Figure 3.2: A single tensor with n indices, represented by n legs. Each leg is represented by μ_k , which run from 1 to D_k , where D_k is the dimension of the Hilbert space endowed on that leg.

where $V_{\mu_1\mu_2\dots\mu_n} |\mu_1\rangle$ is the wavefunction, and the state lives in a Hilbert space $\mathbb{H}_x = \bigotimes_{k=1}^n \mathcal{H}_k$. Now imagine we gather a handful of those tensors and, without making connections between any of them, throw them together, so we have $\bigotimes_x |V_x\rangle$ where x runs over all the nodes.

Next, we build the random tensor network by allowing those tensors to connect through their edges. From now on, for an edge extending from vertex x going into vertex y , we will denote the Hilbert space on this edge as \mathcal{H}_{xy} , and \mathcal{H}_{yx} for the other way around. When we have a dangling edge from vertex x , where the edge is not connected to any vertex, we denote the Hilbert space on this edge as $\mathcal{H}_{x\partial}$ where ∂ means boundary. Note that we assume there to be one dangling leg per boundary vertex. We could have more, but it is the same as gathering all the dangling edges and calling them one.



Figure 3.3: A simple two-tensor network, whose internal leg has dimension D_{xy} , and is projected onto the maximally entangled state in $\mathcal{H}_{xy} \otimes \mathcal{H}_{yx}$

Now for any connected edges, we could see them as a projection to the maximally entangled state. This set up is usually referred to as the projected entangled pair states (PEPS) [29]. Consider the simple case of a two-vertex tensor network (see Figure 3.3). The state for two tensors is $|V_x\rangle \otimes |V_y\rangle$ as defined previously. To connect them, we project them onto the maximally entangled internal leg state $|xy\rangle$, so the result is a state living in the boundary Hilbert state $\mathcal{H}_{x\partial} \otimes \mathcal{H}_{y\partial}$

$$|\Psi\rangle = \langle xy| \left(|V_x\rangle \otimes |V_y\rangle \right) \quad (3.4)$$

To be more generic, we simply let the bras iterate through all internal legs, and let kets be all the tensors in an arbitrary random tensor network.

$$|\Psi\rangle = \bigotimes_{\langle xy \rangle} \langle xy| \left(\bigotimes_x |V_x\rangle \right) \quad (3.5)$$

At this point, we have arrived at a tensor model. To make it random, we simply let each tensor on the vertices $|V_x\rangle$ to Haar randomize before any projection onto internal legs. We could see that the form of bulk to boundary mapping is emerging. To be more precise, we could insert some bulk state to the network. It doesn't have to be a pure state,

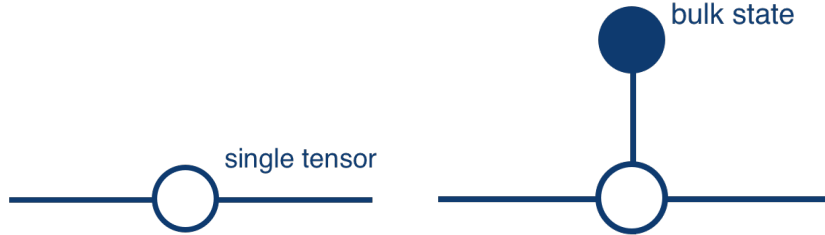


Figure 3.4: Left: single tensor network. Note that we have two dangling legs for one vertex here. A single tensor with one dangling leg would be useless as we want to divide our boundary region into two for entanglement entropy calculation. Right: plugging a bulk state $|\psi_b\rangle$ to the network such that it becomes a kind of bulk to boundary mapping. The bulk state does not have to be a pure state.

in which case we would use the density matrix instead. Let us call it $|\psi_b\rangle$. Together with the contraction between internal legs, we would contract over the bulk states as well.

A baby step for this is the single tensor case(see Figure 3.4), where we plug the bulk state to the single tensor, and since our resulting state lives in the Hilbert space of the dangling legs, it could be considered a mapping from the bulk to the boundary.

A slight improvement to the above will take us to the two-tensor network(see Figure 3.5). In this case, the bulk state is connected to both vertices in the network. We could think of the bulk and the internal leg as a whole, contracted with the tensors on the vertices

$$|\Psi\rangle = \left(\langle\psi_b| \otimes \bigotimes_{\langle xy \rangle} \langle xy| \right) \left(\bigotimes_x |V_x\rangle \right) \quad (3.6)$$

Pictorially, this would be equivalent to the right panel in Figure 3.5. Each tensor is independently mapping the bulk to the boundary legs.

Now since we allow a bulk state that is not pure, it would make more sense to use

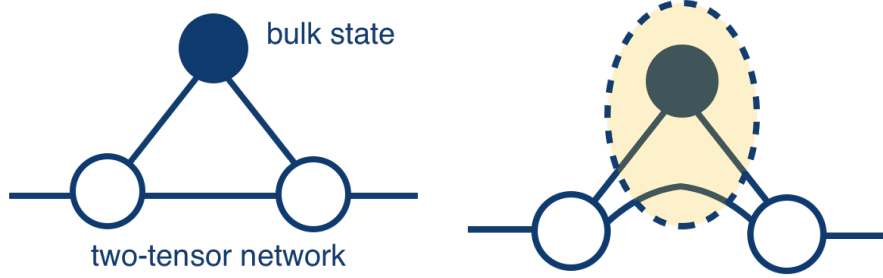


Figure 3.5: Left: a two-tensor network with the bulk state plugged to both tensors. Right: we could combine the internal legs in the network and the bulk state, considering them as one such that effectively the tensors are independently mapping the bulk to respective boundary legs.

density matrix instead. We would then define the following

$$\rho \equiv \text{tr}_P(\rho_P \prod_x |V_x\rangle \langle V_x|) \quad (3.7)$$

$$\rho_P \equiv \rho_b \otimes \bigotimes_{\langle xy \rangle} |xy\rangle \langle xy| \quad (3.8)$$

where we trace over both bulk states and internal legs. We let each $|V_x\rangle$ to randomize, and we would take the average of the above quantity over all states. Since the partial trace is a linear operation, we could perform the averaging before taking the trace.

To randomize each vertex, we would choose a reference state $|0\rangle$ and apply a randomly sampled unitary operator

$$|V_x\rangle = U |0\rangle \quad (3.9)$$

This could be easily done by randomly sampling complex numbers for an n-by-n matrix,

and then orthonormalizing it. This would give us the desired uniform distribution [20]. As a result, the random average of an arbitrary function $f(U|0\rangle)$ is given by

$$\overline{f(U|0\rangle)} = \int dU f(U|0\rangle) \tag{3.10}$$

with $\int dU = 1$. We will next quickly review the swap trick, which will be very helpful as we proceed to calculate a baby step example.

3.3 Swap Trick

In the sections that follow, we will calculate the second Renyi entropy as defined in section 2. We are ultimately interested in the entanglement entropy. However, in our current setup, the Renyi entropy has a flat spectrum [15], which makes the entanglement entropy a free lunch once we have the second Renyi entropy calculated. Flat spectrum is a convenient feature for this calculation and for showing that we can reproduce the Ryu-Takayanagi formula with random tensor network, but it is also a problem that plagues the random tensor network, prohibiting it to reproduce the quantum correction term [12] to the Ryu-Takayanagi formula as described in the Section 2.6. We will touch on this in section ??.

To calculate the second Renyi entropy, a nice trick to have in our pocket is the swap operator trick. First let us imagine we obtain two copies of the same system, each of them is bipartite in the same way, and they don't interact with each other. We write the

composite system

$$|\Psi_1\rangle \otimes |\Psi_2\rangle = \left(\sum_{\alpha_1\beta_1} C_{\alpha_1\beta_1} |\alpha_1\rangle |\beta_1\rangle \right) \otimes \left(\sum_{\alpha_2\beta_2} D_{\alpha_2\beta_2} |\alpha_2\rangle |\beta_2\rangle \right) \quad (3.11)$$

We define a swap operator X_α on subsystem α of each copy, such that it acts on the composite system in the following way

$$X_\alpha |\Psi_1\rangle \otimes |\Psi_2\rangle = X_\alpha \left(\sum_{\alpha_1\beta_1} C_{\alpha_1\beta_1} |\alpha_1\rangle |\beta_1\rangle \right) \otimes \left(\sum_{\alpha_2\beta_2} D_{\alpha_2\beta_2} |\alpha_2\rangle |\beta_2\rangle \right) \quad (3.12)$$

$$= \sum_{\alpha_1\beta_1\alpha_2\beta_2} C_{\alpha_1\beta_1} D_{\alpha_2\beta_2} \left(|\alpha_2\rangle |\beta_1\rangle \otimes |\alpha_1\rangle |\beta_2\rangle \right) \quad (3.13)$$

In this way, the expectation value of the swap operator in the composite system is

$$\langle \Psi \otimes \Psi | X_A | \Psi \otimes \Psi \rangle = \sum_{\alpha_1\beta_1\alpha_2\beta_2} \overline{C_{\alpha_2\beta_1}} C_{\alpha_1\beta_1} \overline{C_{\alpha_1\beta_2}} C_{\alpha_2\beta_2} \quad (3.14)$$

$$= \sum_{\alpha_1,\alpha_2} (\rho_A)_{\alpha_2\alpha_1} (\rho_A)_{\alpha_1\alpha_2} \quad (3.15)$$

$$= \text{tr } \rho_A^2 \quad (3.16)$$

which would relate to the second Renyi entropy through $e^{-S_2(A)} = \frac{\text{tr } \rho_A^n}{(\text{tr } \rho)^n} = \text{tr } \rho_A^n$ supposing that $\text{tr } \rho = 1$ is properly normalized. Note that in the second line we use the fact that

$$\rho = \sum_{\alpha\beta} C_{\alpha\beta} \overline{C_{\alpha\beta}} |\alpha\rangle \langle \alpha| \otimes |\beta\rangle \langle \beta| \quad (3.17)$$

and the density matrix ρ_A of the subsystem A is

$$\rho_A = \text{tr}_B \rho \quad (3.18)$$

$$= \sum_{\alpha\alpha'\beta\beta'\bar{\beta}} C_{\alpha\beta} \overline{C_{\alpha'\beta'}} |\alpha\rangle \langle\alpha'| \otimes \langle\bar{\beta}|\beta\rangle \langle\beta'|\bar{\beta}\rangle \quad (3.19)$$

$$= \sum_{\alpha\alpha'\beta} C_{\alpha\beta} \overline{C_{\alpha'\beta}} |\alpha\rangle \langle\alpha'| \quad (3.20)$$

$$(\rho_A)_{\alpha_1\alpha_2} = \sum_{\alpha\alpha'\beta} C_{\alpha\beta} \overline{C_{\alpha'\beta}} \langle\alpha_1|\alpha\rangle \langle\alpha'|\alpha_2\rangle \quad (3.21)$$

$$= \sum_{\beta} C_{\alpha_1\beta} \overline{C_{\alpha_2\beta}} \quad (3.22)$$

as desired. And we recall that with density matrix, the expectation value of X_A can be expressed as

$$\langle\Psi \otimes \Psi | X_A | \Psi \otimes \Psi\rangle = \text{tr}(\rho \otimes \rho X_A) \quad (3.23)$$

so the second Renyi entropy can be written as

$$e^{-S_2(A)} = \frac{\text{tr}(\rho \otimes \rho X_A)}{\text{tr}(\rho \otimes \rho)} \quad (3.24)$$

3.4 Single Tensor

In this section, we will again consider a single tensor and two dangling legs (see Figure 3.6), each endowed with a Hilbert space with dimension D_A and D_B respectively. One might recall our earlier assumption that each boundary vertex only has one dangling leg.



Figure 3.6: A single tensor with two dangling legs, each endowed with a Hilbert space of dimension D_A and D_B respectively.

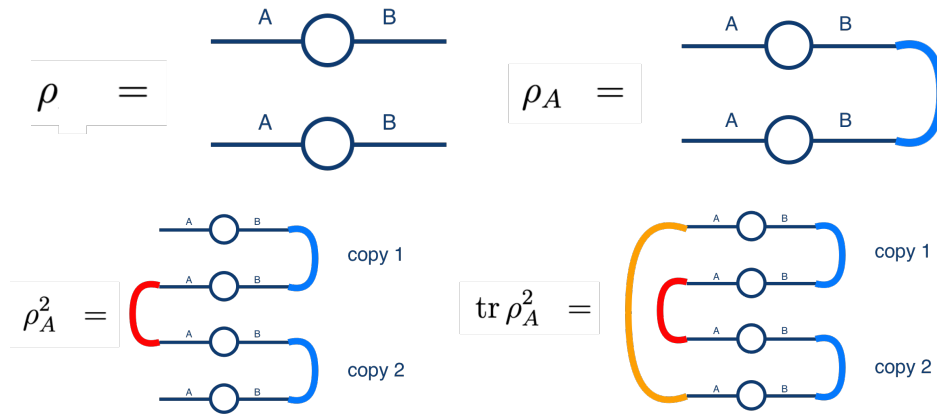


Figure 3.7: A visualization of density matrix and its variations for a single tensor

However, in the case of a single tensor, having only one dangling leg would be pointless – we at least need two to have a bipartite system on the boundary. So naturally, this would be the simplest case to work with. We also note that, while we could have more than two edges for the single tensor, it would be effectively the same when we divide the boundary into two parts.

The quantity we want to calculate is $\text{tr} \rho_A^2$. Recall that one network is one state vector, so a density matrix is represented by two copies of the random tensor network, one for bra and one for ket. This can be visualized with a nice diagram as in Figure 3.7. A visualization like this can help us see why the swap operator works when it is applied to

the random tensor network, at least in a simple case.

We calculate the second Renyi entropy via

$$e^{-S_2(A)} = \frac{\text{tr}(\rho \otimes \rho X_A)}{\text{tr}(\rho \otimes \rho)} \quad (3.25)$$

Note that the swap operator act on the kets. This can be seen easily by recalling the cyclic property within a trace operator. Pictorially, $X_A(\rho \otimes \rho)$ can be visualized with Figure 3.8, where we swap the ket legs of subregion A . When we do the trace $\text{tr} X_A \rho \otimes \rho$, it is represented by Figure 3.9. If we trace the lines in Figure 3.9, we will see this is the same as $\text{tr} \rho_A^2$ in Figure 3.7 once we untangle the lines.

Assuming the density matrix is properly normalized, what we want to calculate is essentially the random average $\overline{\text{tr} \rho \otimes \rho X_A}$, meaning that if we can deal with $\overline{|V\rangle \langle V| \otimes |V\rangle \langle V|}$, we would be all set for this simple case.

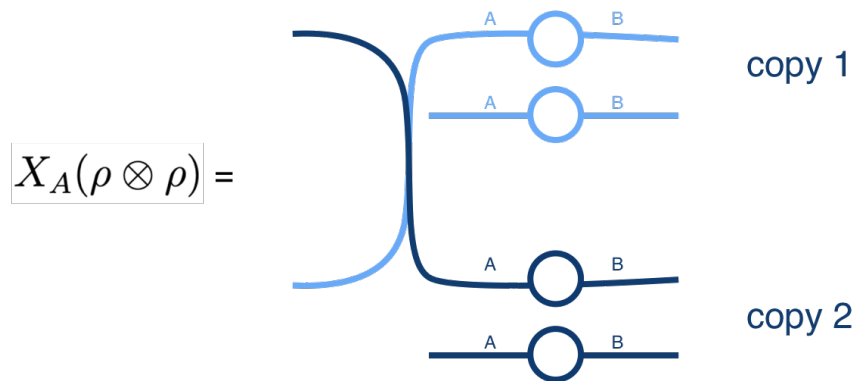


Figure 3.8: Swapping the ket legs of subregion A in the two copies.

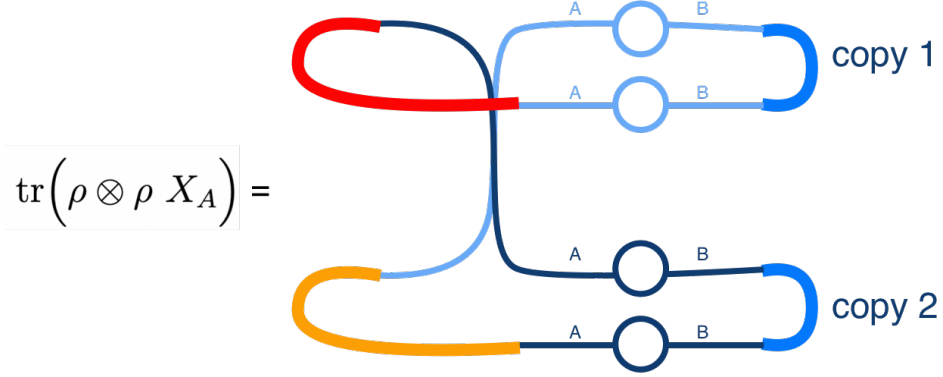


Figure 3.9: Tracing over the networks after the swap operation. We can see that this diagram is the same as Figure 3.7 if we trace the lines.

Let us call $f(U|0\rangle) \equiv |V\rangle\langle V| \otimes |V\rangle\langle V|$. As stated before, the random average is

$$\overline{f(U|0\rangle)} = \int dU f(U|0\rangle) \quad (3.26)$$

This means $\overline{f(U|0\rangle)}$ commutes with all U , so we can write

$$(U \otimes U) \overline{f(U|0\rangle)} (U^\dagger \otimes U^\dagger) = \overline{f(U|0\rangle)} \quad (3.27)$$

We can then apply Schur's lemma [34], such that we can write $\overline{f(U|0\rangle)} = \alpha \mathbb{I} + \beta X$ where \mathbb{I} is the identity and X the swap operator on both subregion A and B , $X \equiv X_A X_B$. Both serve as identity on the $U \otimes U$ space we are working with.

We remind ourselves that $\overline{f(U|0\rangle)}$ is actually an operator. Call it \hat{O} to emphasize this.

With identities $X\hat{O} = \hat{O}$ and $\text{tr } \hat{O} = 1$, we find

$$\alpha = \beta = \frac{1}{D^2 + D} \tag{3.28}$$

where $D \equiv D_A D_B$. In this step we use the fact that trace of the swap operator is $\text{tr } X = D$ while $\text{tr } \mathbb{I} = D^2$. So now we have

$$\text{tr } \overline{\rho \otimes \rho} X_A = \frac{1}{D(D+1)} \text{tr} \left((\mathbb{I} + X) X_A \right) \tag{3.29}$$

$$= \frac{1}{D(D+1)} \text{tr} (X_A + X_B) \tag{3.30}$$

$$= \frac{D_A + D_B}{D + 1} \tag{3.31}$$

$$\approx \frac{1}{D_A} + \frac{1}{D_B} \tag{3.32}$$

where in the last step we assumed $D_A, D_B \gg 1$. The plotted graph for this would be the expectation curve in Figure 3.10, where the scattered dot graph is the numerical result when we randomize the tensor and calculate the entanglement entropy directly through $S_{vN}(A) = -\text{tr } \rho_A \log \rho_A$. And we can see the Page curve is reproduced as expected as we vary the size of one subsystem.

3.5 Large D Limit and Ryu-Takayanagi Formula

To model the physics of AdS/CFT correspondence, an important feature to reproduce is the Ryu-Takayanagi formula. To do this, we will consider again a generic random tensor

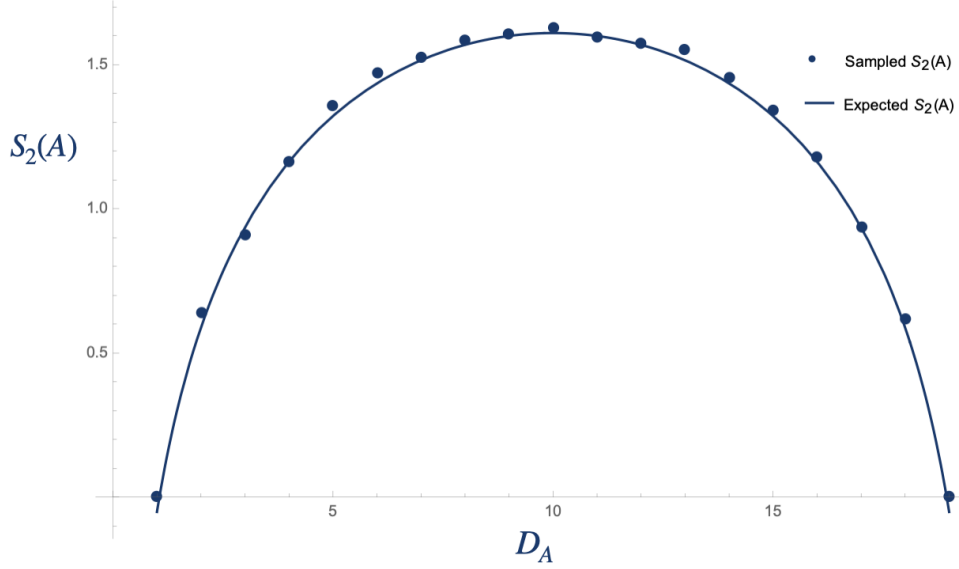


Figure 3.10: Entanglement entropy calculated from randomly sampling the node for a single tensor in comparison to expected Page curve result.

network described by

$$\rho \equiv \text{tr}_P(\rho_P \prod_x |V_x\rangle \langle V_x|) \quad (3.33)$$

$$\rho_P \equiv \rho_b \otimes \bigotimes_{\langle xy \rangle} |xy\rangle \langle xy| \quad (3.34)$$

We will define, for the simplicity of notation,

$$Z_1 \equiv \text{tr}(\rho \otimes \rho X_A) \quad (3.35)$$

$$Z_0 \equiv \text{tr}(\rho \otimes \rho) \quad (3.36)$$

For a large dimension D_{xy} on the internal legs, it is shown that, if we write the above

as $Z_1 = \overline{Z_1} + \delta Z_1$, and the same for Z_0 , the fluctuation could be neglected [15]. We can approximate the second Renyi entropy

$$S_2(A) \approx -\log \frac{\overline{Z_1}}{\overline{Z_0}} \quad (3.37)$$

And this is the reason for us to calculate the random average. We then proceed to plug in the previous expressions for $\overline{Z_1}$

$$\overline{Z_1} = \text{tr} \left(\rho_P \otimes \rho_P \prod_x \overline{|V_x\rangle \langle V_x| \otimes |V_x\rangle \langle V_x| X_A} \right) \quad (3.38)$$

where we trace over internal legs, bulk states, as well as the whole boundary Hilbert space, that is, the dangling legs. Note that we only product over one index x because if we expand the original expression, it would just be two copies of all the density matrices, which we could rearrange into the above form.

We already have from the baby step Section 3.4

$$\overline{|V\rangle \langle V| \otimes |V\rangle \langle V|} = \frac{\mathbb{I} + X}{D(D+1)} \quad (3.39)$$

Plug it into the expression of Z_1 , we have

$$\overline{Z_1} = \frac{1}{\prod_x D_x(D_x+1)} \text{tr} \left(\rho_P \otimes \rho_P \prod_i (\mathbb{I}_i + X_i) X_A \right) \quad (3.40)$$

Now if we expand $\prod_i (\mathbb{I}_i + X_i)$, we can imagine at each site it will either be \mathbb{I} or X , which we can describe using something like bit strings $\{0, 1\}$, and it will be a direct product over

all sites, and summed over all possible variation of the string.

A simple case would be two sites

$$(\mathbb{I}_1 + X_1) \otimes (\mathbb{I}_2 + X_2) = \mathbb{I}_1 \otimes \mathbb{I}_2 + \mathbb{I}_1 \otimes X_2 + X_1 \otimes \mathbb{I}_2 + X_1 \otimes X_2 \quad (3.41)$$

which we can write as $\sum_{\{s_i\}} \prod_i X_i^{\frac{1}{2}(1-s_i)}$, where $s_i \in \{-1, +1\}$ are the spin variables, with -1 being swap operator, and $+1$ being identity at the site. For a tensor network with n vertices, we expect a sum over 2^n terms, each corresponding to a configuration specified by one string of spin variables $\{s_i\}$. With this in mind, we can write

$$\overline{Z}_1 = \frac{1}{\prod_x D_x(D_x + 1)} \text{tr} \left(\rho_P \otimes \rho_P \sum_{\{s_i\}} \prod_i X_i^{\frac{1}{2}(1-s_i)} X_A \right) \quad (3.42)$$

Pull out the sum and define a notion

$$\sum_{\{s_i\}} e^{-\mathcal{A}[\{s_i\}]} \equiv \sum_{\{s_i\}} \frac{1}{\prod_x D_x(D_x + 1)} \text{tr} \left(\rho_P \otimes \rho_P \prod_i X_i^{\frac{1}{2}(1-s_i)} X_A \right) \quad (3.43)$$

With this setup, we can now talk about each configuration separately.

$$\mathcal{A}[\{s_i\}] = -\log \text{tr} \left(\rho_P \otimes \rho_P \prod_i X_i^{\frac{1}{2}(1-s_i)} X_A \right) + \sum_x \log(D_x^2 + D_x) \quad (3.44)$$

Let's think about the first term more closely. As we take the trace over a direct product of two parts, the result will be product of traces over the two parts. Combined with log, we have a sum of *log* terms, one for each part.

The first part will be boundary legs. The trace over dangling legs will either be $D_{x\partial}$ or $D_{x\partial}^2$, depending on whether or not the leg belongs to the subregion A that we are concerned about with our second Renyi entropy $S_2(A)$, and also depends on the spin variable of the vertex connecting to the dangling leg. We can revert back to a two-tensor network to recollect intuition for this statement.

For the two-tensor network (see Figure 3.11), suppose we have the configuration $(-1, +1)$ for site 1 and 2. This will correspond to a configuration of $X_1 \otimes \mathbb{I}_2$. When we compute the Renyi entropy, we will also include the X_A operator in the trace, so the quantity we are interested in is $\text{tr} X_A(X_1 \otimes \mathbb{I}_2)$ for this configuration. To visualize what are being swapped, let us take a look at Figure 3.11. Since the swap operators act on kets, we only put the kets in the diagram to de-crowd the amount of tensor networks in one diagram. When acted by X_1 , the vertices of two copies at site 1 swap, taking both legs with it (recall that $X_1 = X_{1,A}X_{1,B}$). This is illustrated in the mid panel of Figure 3.11. On top of this, if we apply X_A , we get the bottom panel in Figure 3.11. As viewed from the boundary legs, the result (bottom panel) is effectively the same as identity. So when tracing over the boundary leg, we would get $D_{1\partial}^2$ as we have two copies of identities.

The second part is everything inside, which includes both internal legs and bulk states. For this one, we can revert back to the single tensor case (plus a bulk state) to recollect some intuition.

For the single tensor case, we ended up with $\overline{Z}_1 \sim \text{tr} \left((\mathbb{I} + X) X_A \right)$ after random averaging. We would include the bulk state ρ_b and use $\rho_P = \rho_b \otimes \bigotimes_{\langle xy \rangle} |xy\rangle \langle xy|$ as before. There is no internal leg for the single tensor case, but we can still write it anyways, just

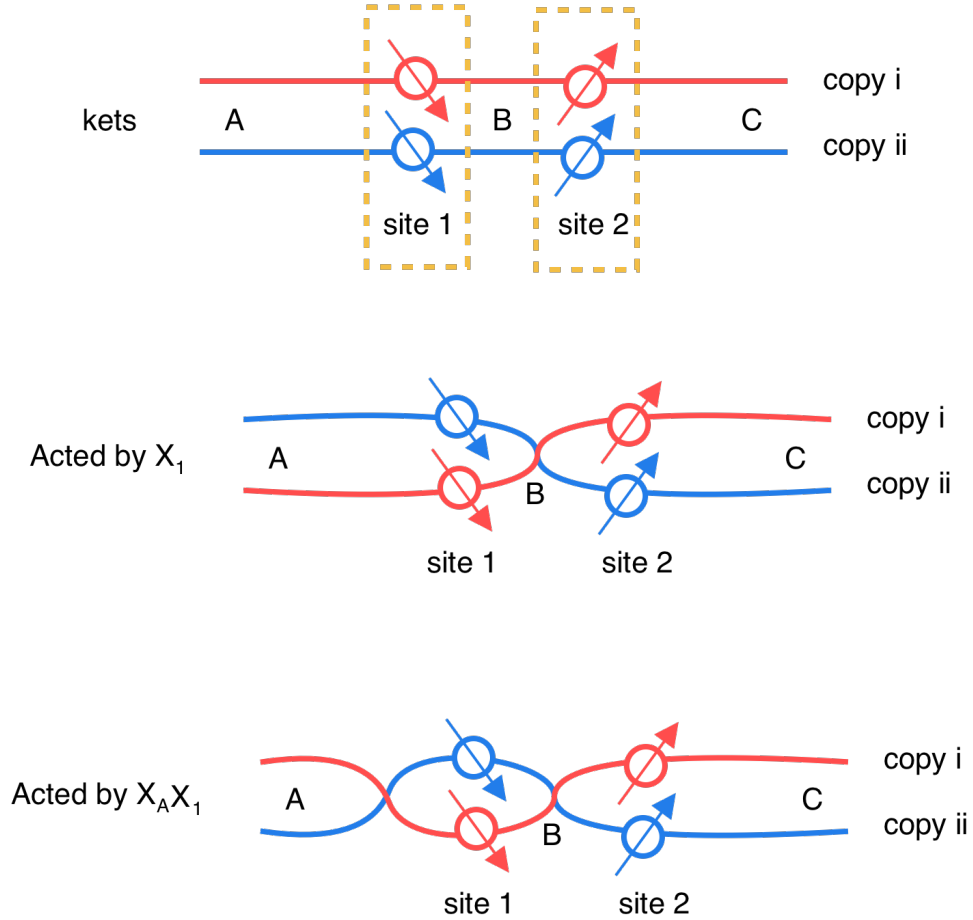


Figure 3.11: Top: the two copies of kets for two-tensor network. Note that in reality we have two copies of density matrices, but we omit the bra here as they are irrelevant here. The swap operators only act on the kets. Middle: the kets as acted on by X_1 the swap operator at site 1. Bottom: the kets as acted on by $X_A X_1$. We see that as viewed from the boundary, this is effectively the same as the top panel. The boundary does not observe the crossing in the boundary leg because no information is shared between the boundary and the boundary nodes, unlike the internal legs, whose information is shared through the projection onto $|xy\rangle$ for nearby nodes x and y . The crossing on the internal leg between site 1 and 2, however, will be seen by both nodes and will be reflected as we take a trace over those.

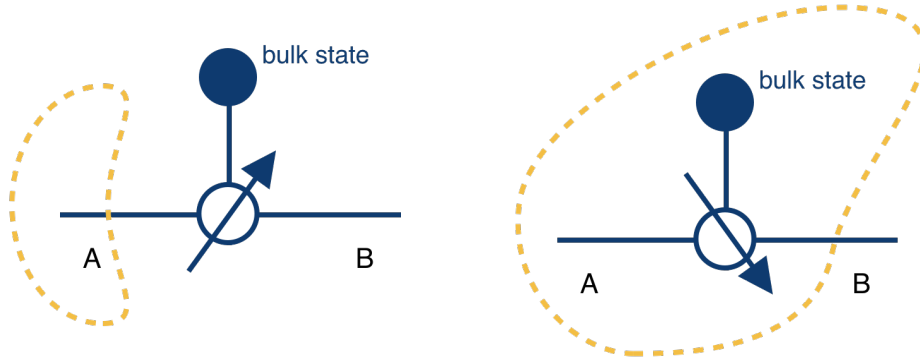


Figure 3.12: Left: single tensor network with bulk state. In this case, identity operator is assigned to the tensor, corresponding to a $s = +1$ spin variable on the tensor. The domain wall is through the dangling leg as we choose A to be the boundary subregion of interest, corresponding to spin down in subregion A . Right: swap operator $s = -1$ is assigned to the tensor, so the domain wall is through the dangling leg of B . In this case, we have $e^{-S_2(A)} \sim \text{tr}(\rho_P \otimes \rho_P X_B)$ so it is effectively the second Renyi entropy of ρ_P restricted to the spin down domain.

to be consistent with notations. In this case, the expression is modified to be

$$\overline{Z}_1 \sim \text{tr}(\rho_P \otimes \rho_P (\mathbb{I} + X) X_A) \quad (3.45)$$

We see there are two terms here, which correspond to the two configurations in Figure 3.12. The first term $\text{tr}(\rho_P \otimes \rho_P X_A)$ is just the second Renyi entropy of ρ_P restricted to the subregion A on the boundary. This term is visualized by the left panel in Figure 3.12, where the spin variation is $s = +1$ as we have \mathbb{I} configuration for the single tensor here. The second term $\text{tr}(\rho_P \otimes \rho_P X X_A) = \text{tr}(\rho_P \otimes \rho_P X_B)$ is visualized in the right panel in Figure 3.12. It is the second Renyi entropy of ρ_P restricted to the entire tensor network excluding the dangling leg B .

With these intuition in mind, we know that

$$\mathcal{A}[\{s_i\}] = -\log \text{tr} \left(\rho_P \otimes \rho_P \prod_i X_i^{\frac{1}{2}(1-s_i)} X_A \right) + \sum_x \log(D_x^2 + D_x) \quad (3.46)$$

can be separated into a boundary leg part, a bulk part defined by the spin down domain, as the constant part with the D_x . For the bulk part, let us use $S_2(\rho_P, s_i = -1)$ to denote the second Renyi entropy of ρ_P restricted to the spin down domain. For the boundary part, us define the variable h_x to decide whether x has a leg in the subregion A .

$$h_x = \begin{cases} +1, x \notin A \\ -1, x \in A \end{cases} \quad (3.47)$$

In this case, when $h_x s_x = +1$, we want $D_{x\partial}^2$; when $h_x s_x = -1$, we want $D_{x\partial}$. We can engineer $D_{x\partial}^{\frac{1}{2}(h_x s_x + 3)}$ to reflect this. Put it all in, we can rearrange the following form.

$$\mathcal{A}[\{s_i\}] = S_2(\rho_P, s_i = -1) - \sum_{x \in \partial} \frac{1}{2} (h_x s_x + 3) \log D_{x\partial} + \sum_x \log(D_x^2 + D_x) \quad (3.48)$$

We remember that the ρ_P is further factorized into the bulk state ρ_b and the internal legs $|xy\rangle\langle xy|$. So we can further separate the $S_2(\rho_P, s_i = -1)$ term into the bulk part $S_2(\rho_b, s_i = -1)$ and the internal leg part, which is just $\log D_{xy}$ when the domain wall is cutting through an internal leg. We shall detail the reason for this latter term.

There are two ways to go about it. First, we can recall the single tensor case. When we choose the boundary leg A to be the subregion of interest and assigning it spin down, we

have two choices of configurations for the tensor. If we choose \mathbb{I} for the tensor, the domain wall is effectively on the dangling leg A (see left panel in Figure 3.12). For this case, we get $\log D_{x\partial}$ for the second Renyi entropy. Dangling leg within A can be treated as another vertex in the spin down domain, so a domain wall crossing through the internal leg should contribute to the entropy similarly, giving $\log D_{xy}$.

We could also calculate it explicitly. Imagine we have two nearby tensors. For simplicity, we could imagine a two-tensor network (see Figure 3.13). We would have

$$S_2(A) \sim \log \text{tr} \left(|12\rangle \langle 12| \otimes |1'2'\rangle \langle 1'2'| (X_1 \otimes \mathbb{I}_2) X_A \right) \quad (3.49)$$

where $|12\rangle$ is the state that lives on the internal leg Hilbert space $\mathcal{H}_{12} \otimes \mathcal{H}_{21}$ and $|1'2'\rangle$ is the second copy. Note that we already pulled out the bulk state portion ρ_b and assigned the operators at each tensor site according to Figure 3.13, hoping to get the $\log D_B = \log(D_{1,B}D_{2,B})$ from this setup.

The above expression can be further treated

$$\sim \log \text{tr} \left(|12\rangle \langle 12| \otimes |1'2'\rangle \langle 1'2'| (X_{1,B} \otimes \mathbb{I}_2) \right) \quad (3.50)$$

$$\sim \log \text{tr} \left(|1'2'\rangle \langle 1'2'| \otimes |12\rangle \langle 12| \right) \quad (3.51)$$

which should then be clear that for the trace to be non-zero, we need to match the 1 and 1'. There are $D_{1,B}$ of those, and $D_{2,B}$ multiplicity of 1, 1' pairs, which makes a count of $D_{1,B}D_{2,B} = D_B$, giving $\log D_B$, which satisfy our claim that the domain wall crossing through internal leg should contribute $\log D_{xy}$ to the second Renyi entropy.

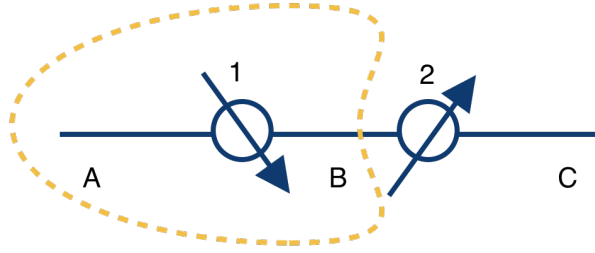


Figure 3.13: Two tensor network with a domain wall cutting through the internal leg. This configuration contributes a $\log D_{xy}$ term to the second Renyi entropy.

With all these, we can further massage the original expression for the entire random tensor network

$$\mathcal{A}[\{s_i\}] = -\frac{1}{2} \left(\sum_{x \in \partial} (h_x s_x - 1) \log D_{x\partial} - \sum_{\langle xy \rangle} (s_x s_y - 1) \log D_{xy} \right) + S_2(\rho_b, s_i = -1) + \text{const.} \quad (3.52)$$

where we throw much of it into the constant pile as they will get canceled out with those in the \overline{Z}_0 term. We can do the similar thing for \overline{Z}_0 except that the boundary will all be spin up. The second Renyi entropy $e^{-S_2(A)}$

With this setup, we map the second Renyi entropy of the random tensor network to the partition function of a classical Ising model defined on the same graph as the tensor network. We see in Equation (3.52) that we have the standard two spin interaction term, and in addition to that, a bulk state term and a term coupling to the boundary field h_x as specified by the subregion A on the boundary. In the case where the bulk state term is small, the contribution will mainly come from the degrees of freedom on the legs, internal and dangling, and $\log D_{xy}$ and $\log D_{x\partial}$ defines an effective notion of temperature of the

Ising model.

Let us then consider the case where all legs have the same degree of freedom $D_{xy} = D_{x\partial} = D$. Then we can define $\beta \equiv \frac{1}{2} \log D$ to be the inverse temperature. Further, if we assume for now the bulk state is a direct-product pure state. This will leave out the ρ_b contribution to the Ising action [15, 22]

$$\mathcal{A}[\{s_i\}] = -\frac{1}{2} \log D \left(\sum_{x \in \partial} (h_x s_x - 1) - \sum_{\langle xy \rangle} (s_x s_y - 1) \right) \quad (3.53)$$

$$(3.54)$$

The part inside the large parenthesis is just counting the number of links the domain wall is cutting through, which is equivalent to a notion of area of the domain wall. Then in the low temperature regime, $\sum_{\{s_i\}} e^{-\mathcal{A}[\{s_i\}]}$ is dominated by the domain wall with minimal area. Assuming the "geodesic" is unique in the random tensor network, we can write

$$S_2(A) \approx \log D \min_{\Sigma \sim A} |\Sigma| \equiv \log D |\gamma_A| \quad (3.55)$$

where the homology constraint is similarly defined as in Section 2 for the derivation of the Ryu-Takayanagi Formula. With this, we have concluded the emergence of Ryu-Takayanagi formula in the random tensor network setup through a mapping to the classical Ising model.

3.6 Going Forward with Random Tensor Network

Albeit successful in many aspects to study holography, random tensor networks remain plagued by a few problems. One of them being the flat spectrum of Renyi entropy

$$S_n = \frac{A}{4G} + S_{n,\text{bulk}} \quad (3.56)$$

where the $\mathcal{O}(G\hbar)^0$ correction term as mentioned in Section 2.6 does not enter. This correction term arises from fluctuations in the background metric and backreaction of multiple extremal surfaces onto each other [6]. Because of this, trying to add an n -dependent term from hindsight would not work, as it would not capture the backreaction of extremal surfaces homologous to disconnected boundary subregions. A possible approach is to consider [2, 5, 9, 13] analysis of entropy on lattice gauge theory. The modification was applied to the HaPPY code in a way that endows extra degrees of freedom to live on the edges [10]. A similar modification is therefore also expected on the random tensor network.

Another concern is the fact that random tensor network is a spatial slice in time. We could write down its state. However, we could not write down its Hamiltonian, that is, we don't know how such a network's time evolution can be computed. It is also argued that random tensor network could not be a natural model for quantum gravity as it violates the uncertainty principle between metric g_{ab} and canonical momentum Π^{ab} [3]. As we choose a time reversal symmetric time slice Σ_0 , the extrinsic curvature $K_{ab} = 0$, leading to $\Pi_{ab} \sim (K_{ab} - g_{ab}K) = 0$. We also have the uncertainty principle

$$[\Pi^{ab}(x), g_{cd}(y)] = -i\delta_{cd}^{ab}\delta(x - y) \quad (3.57)$$

where $\delta_{cd}^{ab} = \frac{1}{2}(\delta_c^a \delta_d^b + \delta_d^a \delta_c^b)$. Now if we want to talk about area, as we would for the Ryu-Takayanagi formula, we will need a well defined notion of metric g_{ab} in Σ_0 . But as we have a precise Π^{ab} , this cannot be achieved. Problems like these remain to be addressed in the future.

References

- [1] Ahmed Almheiri, Thomas Hartman, Juan Maldacena, Edgar Shaghoulian, and Amirhossein Tajdini. The entropy of hawking radiation, 2020.
- [2] Sinya Aoki, Takumi Iritani, Masahiro Nozaki, Tokiro Numasawa, Noburo Shiba, and Hal Tasaki. On the definition of entanglement entropy in lattice gauge theories. Technical report, February 2015. arXiv:1502.04267 [hep-lat, physics:hep-th, physics:quant-ph] type: article.
- [3] Goncalo Araujo-Regado, Rifath Khan, and Aron C. Wall. Cauchy Slice Holography: A New AdS/CFT Dictionary. Technical report, April 2022. arXiv:2204.00591 [gr-qc, physics:hep-th] type: article.
- [4] Luca Bombelli, Rabinder K. Koul, Joochan Lee, and Rafael D. Sorkin. Quantum source of entropy for black holes. *Phys. Rev. D*, 34:373–383, Jul 1986.
- [5] Horacio Casini, Marina Huerta, and Jose Alejandro Rosabal. Remarks on entanglement entropy for gauge fields. *Physical Review D*, 89(8):085012, April 2014. arXiv:1312.1183 [cond-mat, physics:hep-th, physics:quant-ph].

- [6] Xi Dong. The gravity dual of Rényi entropy. *Nature Communications*, 7(1):12472, August 2016.
- [7] Xi Dong and Aitor Lewkowycz. Entropy, extremality, euclidean variations, and the equations of motion. *Journal of High Energy Physics*, 2018(1), Jan 2018.
- [8] Xi Dong, Aitor Lewkowycz, and Mukund Rangamani. Deriving covariant holographic entanglement. *Journal of High Energy Physics*, 2016(11), Nov 2016.
- [9] William Donnelly. Decomposition of entanglement entropy in lattice gauge theory. *Physical Review D*, 85(8):085004, April 2012. arXiv:1109.0036 [cond-mat, physics:gr-qc, physics:hep-lat, physics:hep-th, physics:quant-ph].
- [10] William Donnelly, Donald Marolf, Ben Michel, and Jason Wien. Living on the edge: a toy model for holographic reconstruction of algebras with centers. *Journal of High Energy Physics*, 2017(4), Apr 2017.
- [11] Netta Engelhardt and Aron C. Wall. Quantum extremal surfaces: holographic entanglement entropy beyond the classical regime. *Journal of High Energy Physics*, 2015(1), Jan 2015.
- [12] Thomas Faulkner, Aitor Lewkowycz, and Juan Maldacena. Quantum corrections to holographic entanglement entropy. *Journal of High Energy Physics*, 2013(11), Nov 2013.
- [13] Sudip Ghosh, Ronak M. Soni, and Sandip P. Trivedi. On The Entanglement Entropy For Gauge Theories. *Journal of High Energy Physics*, 2015(9):69, September 2015. arXiv:1501.02593 [cond-mat, physics:hep-th, physics:quant-ph].

- [14] S. W. Hawking. Black hole explosions? *Nature*, 248(5443):30–31, March 1974.
- [15] Patrick Hayden, Sepehr Nezami, Xiao-Liang Qi, Nathaniel Thomas, Michael Walter, and Zhao Yang. Holographic duality from random tensor networks. *Journal of High Energy Physics*, 2016(11), Nov 2016.
- [16] Matthew Headrick. Lectures on entanglement entropy in field theory and holography. Technical report, July 2019. arXiv:1907.08126 [cond-mat, physics:gr-qc, physics:hep-th] type: article.
- [17] Veronika E Hubeny, Mukund Rangamani, and Tadashi Takayanagi. A covariant holographic entanglement entropy proposal. *Journal of High Energy Physics*, 2007(07):062–062, Jul 2007.
- [18] Aitor Lewkowycz and Juan Maldacena. Generalized gravitational entropy. *Journal of High Energy Physics*, 2013(8), Aug 2013.
- [19] Juan Maldacena. The large n limit of superconformal field theories and supergravity. *International Journal of Theoretical Physics*, 38(4):1113–1133, 1999.
- [20] Maris Ozols. How to generate a random unitary matrix. 2009.
- [21] Don N. Page. Average entropy of a subsystem. *Physical Review Letters*, 71(9):1291–1294, Aug 1993.
- [22] Fernando Pastawski, Beni Yoshida, Daniel Harlow, and John Preskill. Holographic quantum error-correcting codes: Toy models for the bulk/boundary correspondence.

- Journal of High Energy Physics*, 2015(6):149, June 2015. arXiv:1503.06237 [hep-th, physics:quant-ph].
- [23] Geoff Penington, Stephen H. Shenker, Douglas Stanford, and Zhenbin Yang. Replica wormholes and the black hole interior, 2020.
- [24] Shinsei Ryu and Tadashi Takayanagi. Aspects of holographic entanglement entropy. *Journal of High Energy Physics*, 2006(08):045–045, Aug 2006.
- [25] Shinsei Ryu and Tadashi Takayanagi. Holographic derivation of entanglement entropy from the anti-de sitter space/conformal field theory correspondence. *Physical Review Letters*, 96(18), May 2006.
- [26] Mark Srednicki. Entropy and area. *Physical Review Letters*, 71(5):666–669, Aug 1993.
- [27] Brian Swingle. Constructing holographic spacetimes using entanglement renormalization. Technical report, September 2012. arXiv:1209.3304 [cond-mat, physics:hep-th, physics:quant-ph] type: article.
- [28] Brian Swingle. Entanglement Renormalization and Holography. *Physical Review D*, 86(6):065007, September 2012. arXiv:0905.1317 [cond-mat, physics:hep-th].
- [29] F. Verstraete and J. I. Cirac. Renormalization algorithms for Quantum-Many Body Systems in two and higher dimensions. Technical report, July 2004. arXiv:cond-mat/0407066 type: article.
- [30] F. Verstraete, J. I. Cirac, and V. Murg. Matrix Product States, Projected Entangled Pair States, and variational renormalization group methods for quantum spin sys-

- tems. *Advances in Physics*, 57(2):143–224, March 2008. arXiv:0907.2796 [cond-mat, physics:math-ph, physics:quant-ph].
- [31] G. Vidal. A class of quantum many-body states that can be efficiently simulated. *Physical Review Letters*, 101(11):110501, September 2008. arXiv:quant-ph/0610099.
- [32] Guifre Vidal. Efficient classical simulation of slightly entangled quantum computations. *Physical Review Letters*, 91(14):147902, October 2003. arXiv:quant-ph/0301063.
- [33] Zhao Yang, Patrick Hayden, and Xiao-Liang Qi. Bidirectional holographic codes and sub-AdS locality. *Journal of High Energy Physics*, 2016(1):175, January 2016. arXiv:1510.03784 [cond-mat, physics:hep-th, physics:quant-ph].
- [34] Anthony Zee. *Group theory in a nutshell for physicists*. Princeton University Press, 2016.